# Antiplasticization and Water Uptake of Nafion Thin Films

**ARTICLE** *in* ACS MACRO LETTERS · FEBRUARY 2012

Impact Factor: 5.76 · DOI: 10.1021/mz200169a



**2 AUTHORS**, INCLUDING:

Shudipto Konika Dishari
Pennsylvania State University
**9** PUBLICATIONS **113** CITATIONS

SEE PROFILE

ACS Macro Letters

Letter

pubs.acs.org/macroletters

# Antiplasticization and Water Uptake of Nafion Thin Films

Shudipto K. Dishari and Michael A. Hickner*

Department of Materials Science and Engineering, The Pennsylvania State University, University Park, Pennsylvania 16802, United States

Supporting Information

**ABSTRACT:** Fluorescence of 9-(2-carboxy-2-cyanovinyl)julolidine (CCVJ) was measured to probe the local motion within 70−600 nm thick Nafion films at controlled levels of hydration. Thinner films showed increased confinement under dry conditions as evidenced by their high fluorescence intensity values per unit thickness. Antiplasticization, or a stiffening of the film, was observed as an increase in fluorescence intensity when the sample was exposed to low water activity (≤30% RH) and the extent of antiplasticization changed with film thickness. At higher relative humidities, the films became plasticized with water and the fluorescence of CCVJ declined. Quartz crystal microbalance (QCM) experiments revealed higher hydration numbers ($\lambda = nH_2O/nSO_3H$) in thinner films on $SiO_2$ surfaces. The higher water uptake in thin films was explained by considering the polymer order at the Nafion−$SiO_2$ interface and the influence of this interfacial layer on the swelling properties of thin films.

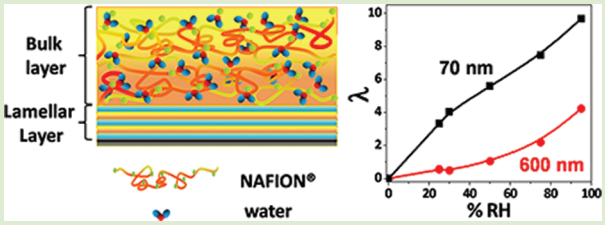


Poly(perfluorosulfonic acid)-based ion-conducting membranes, like Nafion, are the standard material for fuel cells and other electrochemical devices. Extensive work has been undertaken to understand how the structural features of Nafion[1−5] and its water uptake[6−9] influence the material properties of the membrane and ultimately the performance of a cell. There is a large database of information on various forms of Nafion membranes with thicknesses ranging from 20 to 200 $\mu$m, but the properties of thin Nafion thin films (<1 $\mu$m) are relatively unexplored. It is well-established that physical properties of thin polymer films are significantly different compared to their bulk analogs.[10−13] A few reports have focused on the interfacial Nafion−substrate interaction[14−16] and conductivity[17,18] of thin Nafion films, but a clear picture of Nafion's behavior in thin film format has not yet emerged. Systematic investigations of Nafion in the presence of moisture as a function of thickness will be useful in molecular-level understanding of this material's behavior at the catalyst interface.

Usually small molecules act as plasticizers to reduce a polymer's $T_g$, but water can introduce antiplasticization in polymeric systems[19,20] at low moisture content resulting in an increase in polymer modulus. The same film becomes plasticized (less rigid) when water is adsorbed into the material at a higher concentration. Antiplasticization is associated with a decrease in free volume of the polymer leading to a loss of flexibility and segmental mobility of Nafion, as reported by Zhao et al.[9] for thick membranes. Majsztrik et al.[21] reported evidence of stiffening in Nafion membranes at low water activity and high temperature. The stiffening action was believed to be the result of bridging of sulfonic acid groups and hydronium ($H_3O^+$) ions via hydrogen bonding[22−24] at low relative humidity (RH).

Techniques such as NMR,[25] FTIR,[26,27] TGA,[28] and neutron scattering,[29] which have been used to characterize Nafion membranes, are difficult to apply to thin film samples. Moreover, the standard tensile techniques typically employed to measure the mechanical properties of Nafion membranes[9,30] are not applicable to thin films that are difficult to produce in free-standing format. For interrogating thin polymer films, fluorescence-based techniques are attractive due to the high signal intensity of fluorescent probes that are influenced by subtle changes in the polymer. Using a suitable molecular probe sensitive to the hydration environment, fluorescence-based techniques have extracted information on proton dissociation kinetics,[31,32] nanoscopic water environment,[32,33] and water diffusivity[34,35] inside polymer films.

Herein we employed a mobility sensitive fluorescent rotor probe to study the effect of water content on the fluorescence of thin Nafion films. The fluorescence quantum yield of the rotor probe is correlated to the viscosity or mobility of its surrounding environment.[34] In less viscous environments, the increased rotational freedom of the electron donor and acceptor parts of the dye leads to quenching of fluorescence.[36] In this work, thin films were spun cast from a solution containing fluorescent rotor probe 9-(2-carboxy-2-cyanovinyl)julolidine (CCVJ) at a concentration of 0.018% (unless otherwise stated) in Nafion solution. Annealed films with different thicknesses were investigated to measure the effect of confinement on the mobility of the fluorescent dye in the thin films. A custom-built RH control system was integrated with the fluorescence spectrometer to monitor the effect of water activity on the fluorescence response of the spin coated films containing CCVJ. The fluorescence was measured by exciting the dye at a wavelength of 400 nm and the emission spectrum was collected from 420 to 590 nm.

The concentration of CCVJ in the Nafion solution before spin coating was optimized to give the maximum fluorescence

**Received:** November 15, 2011
**Accepted:** January 5, 2012

   dx.doi.org/10.1021/mz200169a | *ACS Macro Lett.* 2012, 1, 291−295

response (Figure S1 in Supporting Information). The thickness-normalized fluorescence intensity ($I_0/L$) at 465 nm of dry films shown in Figure 1 demonstrates significant confinement

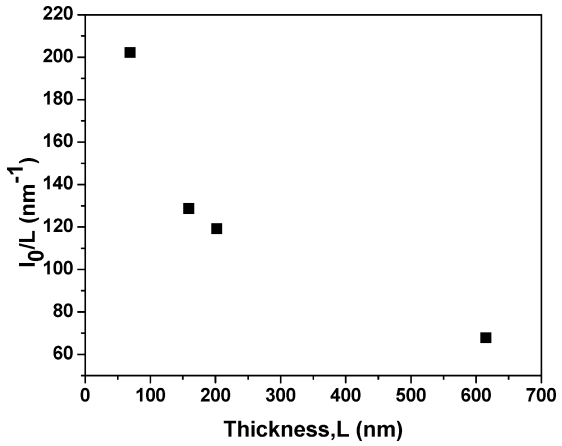


**Figure 1.** Normalized fluorescence intensity ($I_0/L$) of dry film as a function of film thickness ($L$).

as the film thickness decreased. The fluorescence intensity was not a strong function of dye concentration in the thin films (Figure S1), while the fluorescence intensity increased significantly in thinner films, which correlates to stronger confinement effect with decreasing thickness of film as reported.[11]

The fluorescence spectrum of each film was monitored as a function of relative humidity. Figure 2 shows a significant

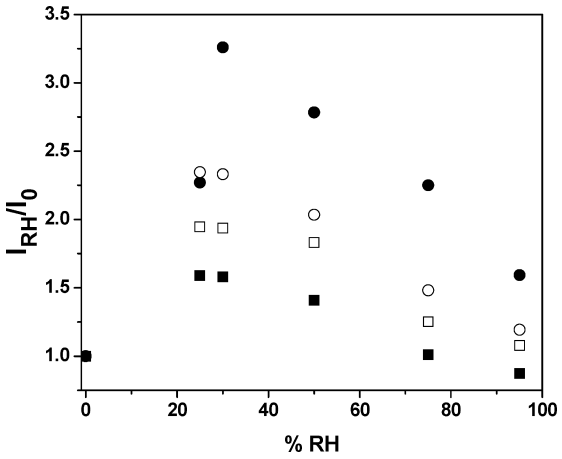


**Figure 2.** Relative fluorescence ($I_{RH}/I_0$) of Nafion films with thicknesses (■) 70, (□) 160, (○) 203, and (●) 616 nm, containing CCVJ as a function of water activity (% RH).

increase in fluorescence for each film at low RH (20–30%). Here $I_{RH}$ represents the fluorescence of the film at a specific RH which was normalized by the fluorescence of the dry film ($I_0$). The fluorescence emission spectrum did not change shape as a function of RH (for the 616 nm film) as shown in Supporting Information (Figure S2).

The increase in fluorescence of the rotor probe at low RH suggested that the surrounding environment restricted the rotational mobility of CCVJ as water was added to the film, thus, increasing the quantum yield and fluorescence intensity. A similar increase in fluorescence intensity was associated with the antiplasticization of polymer matrix as reported by Goodelle et al.[35]

Above 30% RH, the fluorescence started to decrease as high water content plasticized the polymer film. At this point, the distribution of the CCVJ dye in the polymer films has not been measured. CCVJ is polar, so it can be assumed that the dye resides near the interface of the hydrophilic/hydrophobic domains or in the hydrophilic domains in Nafion. As such, the response of the dye is sensitive to the hydration level of the polymer and probes the combined mobility of the polymer and water phases. The fluorescence results were repeatable over three samples with about 10% variability, so it can be assumed that the distribution of dye within the films and the structure of the polymer was consistent over the various experimental runs.

Interestingly, the thinner 70 nm Nafion exhibited a lower degree of antiplasticization than the other samples and the $I_{RH}/I_0$ at low RH steadily increased with increasing film thickness. The large increase in $I_{RH}/I_0$ for a range of dye:polymer ratios in film with thickness of 616 nm (Figure S3) indicated that the extent of antiplasticization was significantly higher in thicker films than in thinner ones, irrespective of the amount of dye in the film. The power-law relationship between fluorescence intensity and viscosity (eq 1) reported by Haidekker et al.[37] can help to quantify the relative change in viscosity of the surrounding environment of CCVJ in film with hydration:

$$\left(\frac{\eta_2}{\eta_1}\right) = \left(\frac{I_2}{I_1}\right)^{1/x} \quad (1)$$

Here, $I$ is the peak fluorescence intensity of rotor probe, $\eta$ is the viscosity of the surrounding medium, and $x$ is the power law exponent. For a probe similar to this work, CCVJ-TEG, $x = 0.52$ was used.[37] Thus, a value of 3.25 for $I_{RH}/I_0$ (616 nm thick film at 30% RH) corresponds to about a 9.6 times increase in viscosity.

The greater value of thickness normalized fluorescence ($I_0/L$) in dry films along with a lower value of $I_{RH}/I_0$ suggests that the thinner film (70 nm) experienced stronger confinement than the thicker samples. The confinement was believed to originate from the polymer–substrate interaction and the layered structure of Nafion adopted at the Si–wafer interface.[15] The water induced less plasticization in the already stiff thin film, but for thicker films with lower stiffness, the antiplasticization was more pronounced.

To further understand the antiplasticization behavior of the Nafion thin films, their hydration was measured as a function of relative humidity using a quartz crystal microbalance (QCM) with $SiO_2$-coated crystals to duplicate the surfaces employed in the fluorescence experiments. The hydration number, $\lambda$, in Figure 3 was calculated as moles of water per mole of sulfonic acid and is proportional to the mass uptake of water in the polymer film for a constant polymer equivalent weight. The hydration of the films increased systematically with decreasing film thickness with the 70 nm film absorbing nearly two times the water of the other films. The high water uptake of the 70 nm film corresponded to its low antiplasticization, whereas the thicker films that had lower hydration numbers experienced greater antiplasticization. The hydration of the films as a function of thickness show a different trend as compared to that reported by Kongkanand for Nafion thin films drop cast on Au.[38] This difference can be attributed to the polymer–substrate interaction for Nafion films on $SiO_2$ and Au, as reported by Dura et al.,[15] and film preparation techniques such as spin coating or drop casting.


dx.doi.org/10.1021/mz200169a | ACS Macro Lett. 2012, 1, 291–295

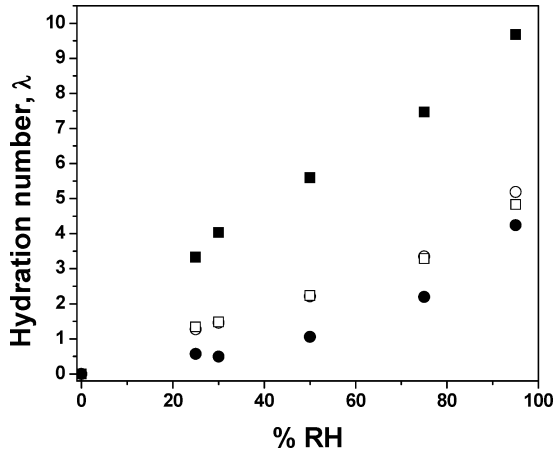


**Figure 3.** Hydration number ($\lambda = n H_2O/n SO_3H$) as a function of relative humidity (% RH) for films with different thicknesses: (■) 70, (□) 160, (○) 203, and (●) 616 nm.

Nafion thin films on $SiO_2$ show an interfacial multilamellar structure composed of water-rich and polymer-rich alternating domains, as demonstrated by Dura et al.[15] This lamellar structure propagated 10 nm from the substrate surface into the film where a bulk-like layer, similar in structure to a membrane with randomly distributed water and polymer domains, was observed in the remainder of the ~50 nm Nafion film. The hydration number of the nonlamellar (bulk) layer on $SiO_2$ reported by Dura et al.[15] ($\lambda \sim 5$, 95% RH) was similar to that obtained in this work by QCM (Figure 3) for thicker films ($\lambda \sim 4$–5, 95% RH) where the bulk layers comprise a significant volume fraction of the film. On the contrary, the lamellar alternating polymer–water layered architecture accounts for the higher hydration number ($\lambda \sim 10$) found in the thinner film (70 nm). Thus, Dura et al.'s[15] structural model can be employed to validate our water uptake results. In addition, the change in the degree of crystallinity with film thickness, not probed in the present work, should also be considered, as crystallinity has connections with film stiffening[39] and water uptake.[40]

To account for the contribution of both the lamellar layer and bulk layer separately in our experiments, we used eq 2 to calculate the $\lambda$ of the film at a specific RH:

$$\lambda_{calc} = (V_{lam} \times \lambda_{lam}) + (V_{bulk} \times \lambda_{bulk}) \quad (2)$$

where $V_{lam}$ and $V_{bulk}$ denote the volume fraction of water in lamellar and bulk layers and $\lambda_{lam}$ and $\lambda_{bulk}$ represent the hydration number of lamellar and bulk layers. For our calculations at 95% RH, $\lambda_{lam}$ was 18.5 (using $\lambda$ of a very thin Nafion film (23 nm) on $SiO_2$ from QCM measurements) and $\lambda_{bulk}$ was taken as 5 on native $SiO_2$, as reported by Dura et al.[15] For an interfacial layer of 22 nm thickness, the hydration number ($\lambda_{calc}$) at 95% RH was calculated from eq 2 to be 5.5 and 9.2 for 616 and 70 nm film, respectively. These $\lambda$ values closely match with the experimentally obtained hydration values by QCM (Figure 3). Moreover, this interfacial layer thickness was comparable to that reported by Dura et al.[15] Thus, this simple physical model of the interfacial structure of Nafion at an $SiO_2$ interface describes the general trends observed in our data and helps to rationalize the water swelling of thin Nafion films. The $\lambda_{calc}$ values at 95% RH were 6.9 for the 160 nm film and 6.5 for the 203 nm film, which are about 30% greater than the measured values. The difficulty in fitting the model described in eq 2 to the 160 and 203 nm thick films could be due to changes in the film structure with thickness, which deserves more study as the trends in hydration with thickness, processing, and surface composition are still to be fully elucidated.

**Scheme 1. Representation of Volume Fraction of the Film Having Lamellar- and Bulk-Like Layers in 616 nm (Top) and 70 nm (Bottom) Film**

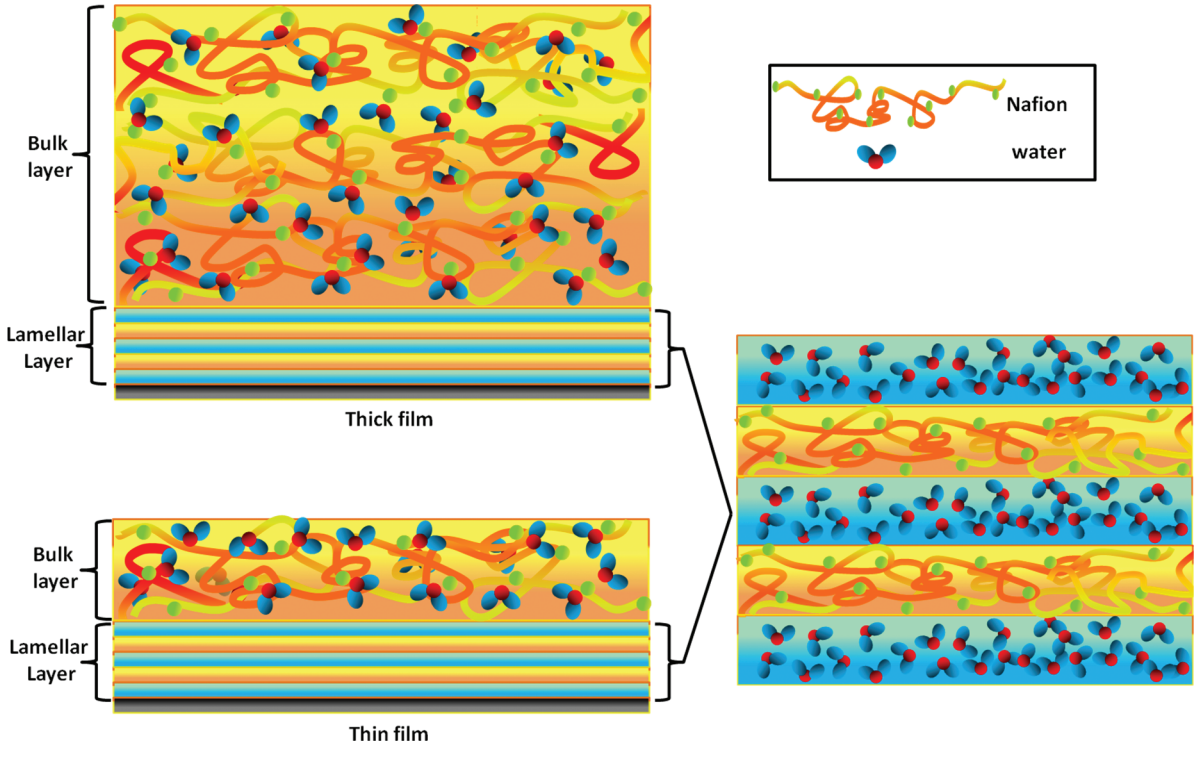



dx.doi.org/10.1021/mz200169a | ACS Macro Lett. 2012, 1, 291–295

In conclusion, fluorescence and water uptake measurements were employed to understand the antiplasticization of thin Nafion films on $SiO_2$ surfaces as a function of water activity. Confinement, as demonstrated by increased fluorescence of a rotor probe, was present for thinner films under dry conditions. Upon exposure to low relative humidity, antiplasticization, or a stiffening of the film, was observed. The interfacial structure of Nafion was reported by Dura, et al.[15] hypothesized to be responsible for the observed trends where thinner films absorbed more water and displayed less antiplasticization than thicker films. By considering the hydration of separate interfacial and bulk layers in the thin films, a simple model was able to account for the differences in hydration of thin films with thicknesses between 70 and 616 nm.

## EXPERIMENTAL METHODS

9-(2-Carboxy-2-cyanovinyl)julolidine, CCVJ, was purchased from Sigma-Aldrich and used as received. A 20% by weight Nafion solution (DE2020, Ion Power, Inc.) was diluted using ethanol to achieve the desired polymer concentrations for spin coating. CCVJ solution in DMSO (5 mg $mL^{-1}$) was added to 10, 5, and 2 wt % Nafion solutions to yield a dye concentration of 0.018 wt %, unless otherwise stated. Silicon wafers were cut into (2 × 2.5 cm) pieces, rinsed with methanol, dried under flowing air, and UV-ozone treated for 20 min. The spin-coating speed was varied along with wt % of Nafion in solution to yield the desired polymer film thicknesses. The thicknesses of the studied films were ∼70 nm (2% Nafion, 3000 rpm), 160 nm (5% Nafion, 5000 rpm), 203 nm (5% Nafion, 3000 rpm), and 616 nm (10% Nafion, 3000 rpm). The films were dried at 42 °C for 3 h under vacuum, annealed at 100 °C for 7 h, and cooled to room temperature for 12 h under vacuum. The thickness of all the films was measured using spectroscopic ellipsometry at ambient conditions. These thickness values matched well with those calculated from QCM results, assuming a polymer density of 2.0 g $cm^{-3}$. A custom-built RH control system was connected to a Photon Technology International, Inc. (Birmingham, NJ) QuantaMaster fluorimeter to produce a sample environment with specific water activity. Air at dewpoint was produced by a sparging system. The dewpoint humidified wet air was mixed with a stream of dry air and the flow rates of the wet and dry streams were varied to achieve a specific relative humidity. A RH probe was connected to the gas outlet from the fluorescence humidity chamber for in situ monitoring of the relative humidity of the sample environment.

## ASSOCIATED CONTENT

### Supporting Information

Experimental details of film preparation and measurements of RH-dependent fluorescence. This material is available free of charge via the Internet at http://pubs.acs.org.

## AUTHOR INFORMATION

### Corresponding Author

*E-mail: hickner@matse.psu.edu. Tel.: 814-933-2204. Fax: 814-865-2917.

### Notes

The authors declare no competing financial interest.

## ACKNOWLEDGMENTS

The authors acknowledge the support of the U.S. Department of Energy, the Office of Energy Efficiency and Renewable Energy, the Fuel Cells Technology Program through a subcontract from General Motors Corporation under Grant DE-EE0000470.

## REFERENCES

(1) Gierke, T. D.; Munn, G. E.; Wilson, F. C. *J. Polym. Sci.: Polym. Phys. Ed.* **1981**, *19*, 1687−1704.
(2) Mauritz, K. A.; Moore, R. B. *Chem. Rev.* **2004**, *104*, 4535−4585.
(3) Spry, D. B.; Goun, A.; Glusac, K.; Moilanen, D. E.; Fayer, M. D. *J. Am. Chem. Soc.* **2007**, *129*, 8122−8130.
(4) Kreuer, K. D. *J. Membr. Sci.* **2001**, *185*, 29−39.
(5) Boakye, E. E.; Yeager, H. L. *J. Membr. Sci.* **1992**, *69*, 155−167.
(6) Morris, D. R.; Sun, X. *J. Appl. Polym. Sci.* **1993**, *50*, 1445−1452.
(7) Majsztrik, P.; Bocarsly, A.; Benziger, J. *J. Phys. Chem. B* **2008**, *112*, 16280−16289.
(8) Krtil, P.; Trojanek, A.; Samec, Z. *J. Phys. Chem. B* **2001**, *105*, 7979−7983.
(9) Zhao, Q.; Majsztrik, P.; Benziger, J. *J. Phys. Chem. B* **2011**, *115*, 2717−2727.
(10) Beaucage, G.; Composto, R.; Stein, R. S. *J. Polym. Sci., Part B: Polym. Phys.* **1993**, *31*, 319−326.
(11) Forrest, J. A.; Dalnoki-veress, K. *Adv. Colloid Interface Sci.* **2001**, *94*, 167−196.
(12) Frank, B.; Gast, A. P.; Russel, T. P.; Brown, H. R.; Hawker, C. *Macromolecules* **1996**, *29*, 6531−6534.
(13) Keddie, J. L.; Jones, R. A. L.; Cory, R. A. *Faraday Discuss.* **1994**, *98*, 219−230.
(14) Noguchi, H.; Taneda, K.; Minowa, H.; Naohara, H.; Uosaki, K. *J. Phys. Chem. C* **2010**, *114*, 3958−3961.
(15) Dura, J. A.; Murthi, V. S.; Hartman, M.; Satija, S. K.; Majkrzak, C. F. *Macromolecules* **2009**, *42*, 4769−4774.
(16) Wood, D. L.; Chlistunoff, J.; Majewski, J.; Borup, R. L. *J. Am. Chem. Soc.* **2009**, *131*, 18096−18104.
(17) Paul, D. K.; Fraser, A.; Karan, K. *Electrochem. Commun.* **2011**, *13*, 774−777.
(18) Siroma, Z.; Kakitsubo, R.; Fujiwara, N.; Ioroi, T.; Yamazaki, S.-ichi; Yasuda, K. *J. Power Sources* **2009**, *189*, 994−998.
(19) Seow, C. C.; Cheah, P. B.; Chang, Y. P. *J. Food Sci.* **1999**, *64*, 576−581.
(20) Chang, Y. P.; Cheah, P. B.; Seow, C. C. *J. Food Sci.* **2002**, *67*, 3396−3401.
(21) Majsztrik, W.; Bocarsly, A. B.; Benziger, J. B. *Macromolecules* **2008**, *41*, 9849−9862.
(22) Bauer, F.; Denneler, S.; Willert-Porada, M. *J. Polym. Sci., Part B: Polym. Phys.* **2005**, *43*, 786−795.
(23) Laporta, M.; Pegoraro, M.; Zanderighi, L. *Phys. Chem. Chem. Phys.* **1999**, 4619−4628.
(24) Roussenova, M.; Murith, M.; Alam, A.; Ubbink, J. *Biomacromolecules* **2010**, *11*, 3237−47.
(25) Guillermo, A.; Gebel, G.; Mendil-Jakani, H.; Pinton, E. *J. Phys. Chem. B* **2009**, *113*, 6710−6717.
(26) Korzeniewski, C.; Snow, D. E.; Basnayake, R. *Appl. Spectrosc.* **2006**, *60*, 599−604.
(27) Hallinan, D. T.; Elabd, Y. a *J. Phys. Chem. B* **2009**, *113*, 4257−66.
(28) Wang, Y.; Kawano, Y.; Aubuchon, S. R.; Palmer, R. a *Macromolecules* **2003**, *36*, 1138−1146.
(29) Xu, F.; Diat, O.; Gebel, G.; Morin, A. *J. Electrochem. Soc.* **2007**, *154*, B1389−B1398.
(30) Satterfield, M. B.; Majsztrik, P. W.; Ota, H.; Benziger, J. A. Y. B.; Bocarsly, A. B. *J. Polym. Sci., Part B: Polym. Phys.* **2006**, *44*, 2327−2345.
(31) Spry, D. B.; Fayer, M. D. *J. Phys. Chem. B* **2009**, *113*, 10210−10221.
(32) Spry, D. B.; Goun, A.; Glusac, K.; Moilanen, D. E.; Fayer, M. D. *J. Am. Chem. Soc.* **2007**, *129*, 8122−8130.
(33) Satpati, A. K.; Kumbhakar, M.; Nath, S.; Pal, H. *Chem. Phys. Chem.* **2009**, *085*, 2966−2978.
(34) Ellison, C. J.; Miller, K. E.; Torkelson, J. M. *Polymer* **2004**, *45*, 2623−2632.
(35) Goodelle, J. P.; Pearson, R. A.; Santore, M. M. *J. Appl. Polym. Sci.* **2002**, *86*, 2463−2471.
(36) Haidekker, M. A.; Theodorakis, E. A. *J. Biol. Eng.* **2010**, *4*, 1−14.

(37) Haidekker, M. A.; Brady, T. P.; Lichlyter, D.; Theodorakis, E. A. *Bioorg. Chem.* **2005**, *33*, 415−425.
(38) Kongkanand, A. *J. Phys. Chem. C* **2011**, *115*, 11318−11325.
(39) Benziger, J.; Bocarsly, A.; Cheah, M. J.; Majsztrik, P. *Struct. Bond.* **2011**, *141*, 85−113.
(40) Huang, H.; Xu, Y.; Low, H. Y. *Polymer* **2005**, *46*, 5949−5955.